JACS
JOURNAL OF THE AMERICAN CHEMICAL SOCIETY
Communication
pubs.acs.org/JACS

Design of Efficient Thermally Activated Delayed Fluorescence Materials for Pure Blue Organic Light Emitting Diodes

Qisheng Zhang,[†] Jie Li,[†] Katsuyuki Shizu,[†] Shuping Huang,[‡] Shuzo Hirata,[†] Hiroshi Miyazaki,[†] and Chihaya Adachi*[,†]

[†]Center for Organic Photonics and Electronics Research (OPERA) and [‡]Institute for Materials Chemistry and Engineering, Kyushu University, 744 Motooka, Nishi-ku, Fukuoka 819-0395, Japan

Supporting Information

ABSTRACT: Efficient thermally activated delayed fluorescence (TADF) has been characterized for a carbazole/sulfone derivative in both solutions and doped films. A pure blue organic light emitting diode (OLED) based on this compound demonstrates a very high external quantum efficiency (EQE) of nearly 10% at low current density. Because TADF only occurs in a bipolar system where donor and acceptor centered $^3\pi\pi^*$ states are close to or higher than the triplet intramolecular charge transfer (^{3}CT) state, control of the π-conjugation length of both donor and acceptor is considered to be as important as breaking the π-conjugation between them in blue TADF material design.

Organic light emitting diodes (OLEDs) containing Ir(III), Pt(III), or Os(II) based phosphors can harvest both singlet (25%) and triplet (75%) excitons through heavy atom enhanced intersystem crossing (ISC), and therefore approach an external electroluminescence (EL) quantum efficiency (EQE) that is 4 times higher than that of conventional fluorescent OLEDs.[1] However, the high cost of these phosphors hinders the prospective application of these devices in many fields, including mobile displays, large-screen displays, and general lighting. The development of low cost substitutes for these noble metal-based phosphors has attracted increasing attention over the past decade. In 2006, Wang's group demonstrated green EL devices based on a Cu(I) complex that could achieve an EQE as high as 16%, indicating that both the triplet and singlet excitons generate light in these devices.[2] Subsequently, highly efficient EL from Cu(I) complexes was also confirmed in some other Cu(I) systems.[3] Because the radiative decay rate of a triplet state is less favorable for the first row transition metal complexes, the emission from these Cu(I) complexes was believed to arise from an upper state which is in thermal equilibrium with the lowest triplet state and involves some singlet characters. In principle, when the energy difference (ΔE_{ST}) between the lowest singlet state (S_1) and the lowest triplet state (T_1) is small, reverse ISC can take place even in pure aromatic organic compounds containing no heavy metals.[4] A small overlap between the highest occupied and lowest unoccupied molecular orbitals (HOMO and LUMO) is considered to be an important factor in realization of the small ΔE_{ST}.[1b,5] On the basis of this concept, several efficient green emitting thermally activated delayed fluorescence (TADF) molecules have recently been designed and used successfully to improve the light emitting capability of OLEDs by our group.[6] Thus, pure organic TADF materials take on the advantages of chemical and thermal stability as compared to those luminescent Cu(I) complexes, allowing them to be designed, synthesized, and applied more easily in OLEDs.

In this paper, we report on one promising type of pure blue TADF material and its design principle. The formulas of the compounds discussed here are depicted in Figure 1. Reaction of

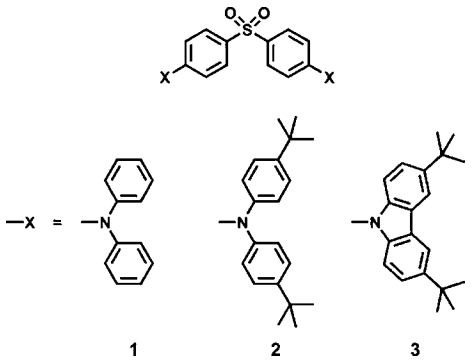

Figure 1. Molecular structures of compounds **1**−**3**.

diphenylamine, bis(4-*tert*-butylphenyl)amine or 3,6-di-*tert*-butylcarbazole, with sodium hydride and bis(4-fluorophenyl)-sulfone produces good yields of the compounds (SI section 3). The absorption and emission spectra of these compounds in low polar toluene are shown in Figure 2. At room temperature, all three compounds exhibit broad and structureless emission bands with a maximum at 402−419 nm, which can be ascribed to the intramolecular charge-transfer (CT) transition because of their dipolar nature. In contrast, their phosphorescence spectra at 77 K are well resolved and show a characteristic vibrational structure for triphenylamine or 9-phenylcarbazole (see Figure S3), indicating that their T_1 states are $^3\pi\pi^*$ states located mostly on the electron donating moieties. For the $^3\pi\pi^*$ state, the highest energy peak of its emission identifies its zero−zero energy (E_{0-0}). However, for a CT state without any vibronic structure, estimation of E_{0-0} from the onset of its broad emission band provides a more comparable result, as demonstrated by some previous studies.[3d,7] From Figure 2, the

Received: July 4, 2012
Published: August 29, 2012

   dx.doi.org/10.1021/ja306538w | J. Am. Chem. Soc. 2012, 134, 14706−14709

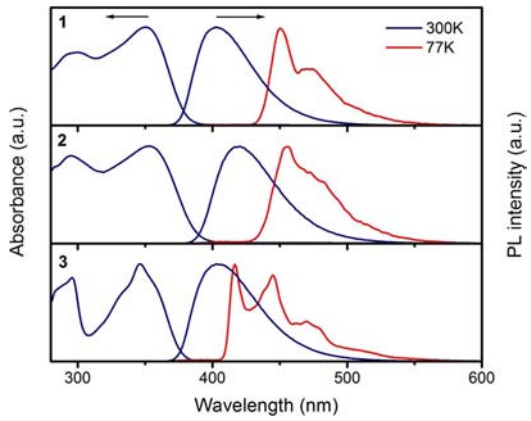

Figure 2. Absorption and emission spectra of compounds **1**–**3** in toluene at 300 K and their phosphorescence spectra (delayed by 10 ms) in toluene at 77 K.

ΔE_{ST} values of compounds **1**, **2**, and **3** are calculated to be 0.54, 0.45, and 0.32 eV, respectively. This change in ΔE_{ST} can be explained well in terms of the modification of the molecular structures. The introduction of *tert*-butyl groups on the diphenylamine unit enhances its electron donating ability, and consequently lowers the CT energy and the ΔE_{ST}. On the other hand, the replacement of a diphenylamine unit with a carbazole unit slightly raises the ^{1}CT state, and considerably raises the $^3\pi\pi^*$ state, resulting in a further decrease in its ΔE_{ST}.

Time dependent density functional theory (TD-DFT) calculations can also predict the ΔE_{ST} changes of these three compounds. Using the most popular B3LYP density functional, the ΔE_{ST} values of **1**, **2**, and **3** were calculated to be 0.65, 0.60, and 0.34 eV, respectively, based on their ground state geometries when optimized by the DFT (B3LYP/6-31G*) method. These results are well matched with the experimental values. The electron densities of the HOMO and LUMO of each of these three compounds are depicted in Figures 3 and

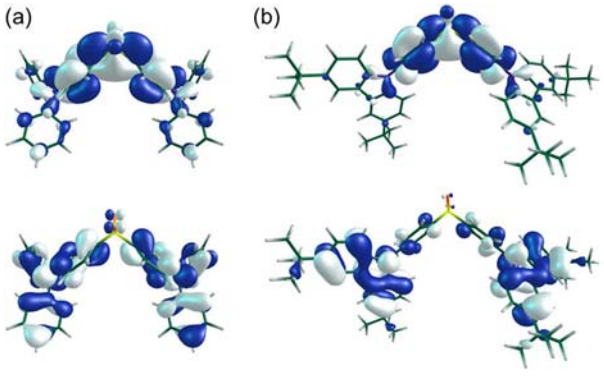

Figure 3. The HOMO (lower image) and LUMO (upper image) of compounds **1** (a) and **3** (b) calculated at the B3LYP/6-31G* level. The calculated S_1/T_1 energies of **1** and **3** are 3.54/2.89 eV and 3.31/2.97 eV, respectively, corresponding to the measured values of 3.30/2.76 eV and 3.30/2.98 eV, respectively.

S4. In comparison with the phenylamine derivatives, **1** and **2**, the carbazole derivative **3** shows a greater separation of the HOMO and LUMO orbitals because of the relatively large dihedral angle of 49° between the phenyl bridge and the donor moiety, in contrast with that of ~32° for **1** and **2**. The lower overlap between the HOMO and the LUMO of **3** indicates a smaller energy difference between its singlet and triplet CT states.

The photoluminescence quantum yields (PLQY) of **1**, **2**, and **3** in oxygen-free toluene are 0.57, 0.65, and 0.69, respectively. The transient photoluminescence (PL) decay characteristics of these solutions show two-component decays, that is, a fast decay with a lifetime of 3–5 ns and a slow decay with a lifetime of 90–270 μs (see Table S1), which can be assigned to fluorescence and TADF decay, respectively. The proportion of the slow decay component decreases with an increase in the ΔE_{ST} of these compounds, and almost disappears in the case of **1** (Figure 4). Similar to the case of our previous report,[6a] the

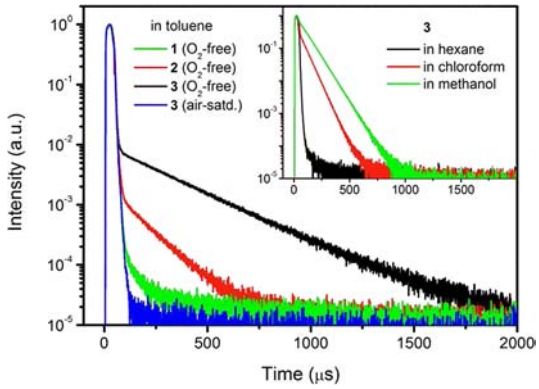

Figure 4. Emission decay of compounds **1**–**3** in toluene at 300 K. Inset: Emission decay of **3** in oxygen-free hexane, chloroform, and methanol at 300 K.

slow decay component cannot be observed in an air-equilibrated solution as a consequence of oxygen quenching. Here, the observed TADF emission is believed to occur through a mechanism that involves a reverse internal conversion (IC) from the donor centered $^3\pi\pi^*$ state to the ^{3}CT state and a successive reverse ISC from the ^{3}CT state to the ^{1}CT state. The reversible energy transfer between the $^3\pi\pi^*$ and ^{3}CT states can be regarded as a rapid intramolecular electron exchange process, and has been demonstrated by some transition metal CT complexes with an energy separation of less than 0.20 eV between the two states.[3d,8] Similar to the reversible ISC process,[6b] the energy difference between $E_{0-0}(^3\text{CT})$ and $E_{0-0}(^3\pi\pi^*)$ determines the reverse IC rate.

The photophysical properties of **3** were also measured in various solvents with different polarities. In the polar solvents chloroform and methanol, the emission maximum red-shifts to 446 and 469 nm (Figure S5a), respectively, and the lifetime of the slow decay decreases dramatically to 56 and 83 μs (Figure 4 inset), respectively, compared to the values of 404 nm and 270 μs in toluene. Conversely, in the nonpolar solvent hexane, the emission maximum blue-shifts (Figure S5a), while the slow decay component disappears (Figure 4 inset). To explain this change in emission decay, we consider that a CT state with a large dipole moment change is more easily stabilized by a polar solvent with respect to the $\pi\pi^*$ state, leading to an approach to or inversion of the ^{3}CT and $^3\pi\pi^*$ states. The increased CT characteristics of its phosphorescence spectra in chloroform and methanol glasses at 77 K (Figure S5b) implies that the ^{3}CT state might be the lowest triplet state for **3** in these two solvents at 300 K, when taking the growing solvation in a fluid solution into account. Because of the lack of a reversible IC process, the energy up-conversion from the T_1 state to the S_1 state becomes

dx.doi.org/10.1021/ja306538w | J. Am. Chem. Soc. 2012, 134, 14706–14709

much faster in a polar solvent. In contrast, the difference between $E_{0-0}(^3\mathrm{CT})$ and $E_{0-0}(^3\pi\pi^*)$ increases in nonpolar hexane solvent, and as a result, the reverse IC process is hindered and the total PLQY (0.52) is thus lower than that in the three other solvents (~0.70).

By doping of these three compounds in a high triplet energy host, bis(2-(diphenylphosphino)phenyl)ether oxide (DPEPO), with a concentration of 10 wt %, the TADF emissions were also observed in vacuum conditions. The proportion of the delayed component in the total emission occurs in the order **3** > **2** > **1** (see Figure S7), which agrees with the behavior in toluene. The emission maximum and the PLQY of **1**, **2**, and **3** in the DPEPO films are 421 nm/0.60, 430 nm/0.66, and 423 nm/0.80, respectively. Using these doped DPEPO films as the emitting layers (EML), multilayer OLEDs were fabricated with a configuration of ITO/α-NPD (30 nm)/TCTA (20 nm)/CzSi (10 nm)/EML (20 nm)/DPEPO (10 nm)/TPBI (30 nm)/LiF (1 nm)/Al (Figure S8), where α-NPD, TCTA, CzSi and TPBI represent *N*,*N*′-diphenyl-*N*,*N*′-bis(1-naphthyl)-1,10-biphenyl-4,4′-diamine, 4,4′,4″-tris(*N*-carbazolyl) triphenylamine, 9-(4-*tert*-butylphenyl)-3,6-bis(triphenylsilyl)-9*H*-carbazole and 1,3,5-tris(*N*-phenylbenzimidazol-2-yl)benzene, respectively. As shown in Figure 5a, the maximum EQE of the device based on **1** is 2.9%, while the values for the devices based on **2** and **3** increase dramatically to 5.6% and 9.9%, respectively, although the EQE roll-off of all these devices is significant, probably because of the unbalanced charge capture ability of these large band gap emitters in the EML. The EL spectra of these devices are almost identical to the PL spectra of their EMLs (Figures 5b and S9). The Commission Internationale de L'Eclairage (CIE) coordinates of the EL of the **3**-based device are (0.15, 0.07), which are very close to those of the National Television Standards Committee (NTSC) standard blue of (0.14, 0.08). Note that a pure blue fluorescent OLED generally has an EQE of less than 3%,[9] and pure blue emission with CIE_y < 0.10 is still a critical issue for phosphorescent transition-metal complexes.[10] Here, $\mathrm{Ir(fppz)_2(dfbdp)}$[10e] was selected for comparison because it is the most efficient blue phosphor, with a strong emission band in the 400−450 nm region. Using the same configuration described above, an $\mathrm{Ir(fppz)_2(dfbdp)}$ based device exhibits a similar maximum EQE of 8.8% with a reduced efficiency roll-off when compared with that of the **3**-based device (see Figure S10). We believe that the design of an appropriate device structure in a subsequent study can solve the roll-off problem.

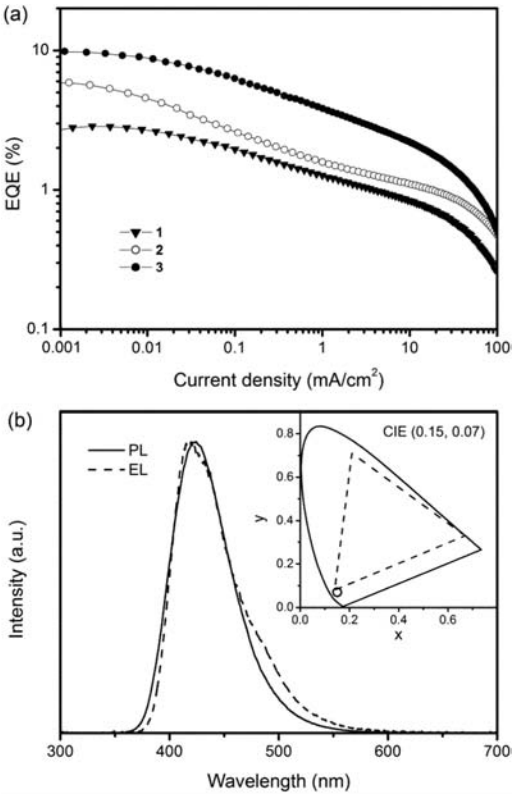

Figure 5. (a) The EQE-current density characteristics of the OLEDs based on compounds **1**−**3**; (b) the EL and PL spectra of 10 wt % **3** doped in a DPEPO layer. Inset: The CIE coordinates of the EL spectrum of a **3**-based device.

In summary, although a high degree of CT in the excitation process leads to a small exchange energy between the singlet and triplet CT states, the $^3\pi\pi^*$ state is the lowest triplet state for an aromatic CT compound in most cases. The energy interchange between its singlet and triplet states can be efficient only when the $^3\pi\pi^*$ state is close to or even higher than the ^{3}CT state. Therefore, to attain efficient blue TADF emission, both the π-conjugation length and the redox potential of the donor and acceptor moieties should be taken into account, along with the interruption of the conjugation between them. On the basis of this principle, a simple and efficient pure blue TADF material has been designed and successfully applied to OLEDs. Its higher EL efficiency relative to fluorescent materials with similar CIE coordinates indicates that TADF materials have great potential for OLED applications, even in the pure blue region where noble metal based phosphors do not work well.

■ ASSOCIATED CONTENT

Supporting Information

Experimental details; photophysical and molecular orbital data; comparison of device data. This material is available free of charge via the Internet at http://pubs.acs.org.

■ AUTHOR INFORMATION

Corresponding Author

adachi@cstf.kyushu-u.ac.jp

Notes

The authors declare no competing financial interest.

■ ACKNOWLEDGMENTS

The authors wish to thank Prof. Masahiro Kotani for stimulating discussions with regard to this work. This work was supported by a Grant-in-Aid from the Funding Program for World-Leading Innovative R&D on Science and Technology (FIRST).

■ REFERENCES

(1) (a) Adachi, C.; Baldo, M. A.; Thompson, M. E.; Forrest, S. R. *J. Appl. Phys.* **2001**, *90*, 5048. (b) *Highly Efficient OLEDs with Phosphorescent Materials*; Yersin, H., Ed.; Wiley-VCH, Weinheim, 2008. (c) Xiao, L.; Chen, Z.; Qu, B.; Luo, J.; Kong, S.; Gong, Q.; Kido, J. *Adv. Mater.* **2011**, *23*, 926.

(2) Zhang, Q.; Zhou, Q.; Cheng, Y.; Wang, L.; Ma, D.; Jing, X.; Wang, F. *Adv. Funct. Mater.* **2006**, *16*, 1203.

(3) (a) Tsuboyama, A.; Kuge, K.; Furugori, M.; Okada, S.; Hoshino, M.; Ueno, K. *Inorg. Chem.* **2007**, *46*, 1992. (b) Deaton, J. C.; Switatski, S. C.; Kondakov, D. Y.; Young, R. H.; Pawlik, T. D.; Giesen, D. J.;

Harkins, S. B.; Miller, A. J. M.; Mickenberg, S. F.; Peters, J. C. *J. Am. Chem. Soc.* **2010**, *132*, 9499. (c) Hashimoto, M.; Igawa, S.; Yashima, M.; Kawata, I.; Hoshino, M.; Osawa, M. *J. Am. Chem. Soc.* **2011**, *133*, 10348. (d) Zhang, Q.; Komino, T.; Huang, S.; Matsunami, S.; Goushi, K.; Adachi, C. *Adv. Funct. Mater.* **2012**, *22*, 2327.

(4) Valeur, B. *Molecular Fluorescence Principles and Applications*; Wiley-VCH: Weinheim, 2002; p 41.

(5) Klessinger, M.; Michl, J. *Excited States and Photochemistry of Organic Molecules*; VCH: Weinheim, 1995.

(6) (a) Endo, A.; Sato, K.; Yoshimura, K.; Kai, T.; Kawada, A.; Miyazaki, H.; Adachi, C. *Appl. Phys. Lett.* **2011**, *98*, 083302. (b) Goushi, K.; Yoshida, K.; Sato, K.; Adachi, C. *Nat. Photonics* **2012**, *6*, 253. (c) Nakagawa, T.; Ku, S.-Y.; Wong, K.-T.; Adachi, C. *Chem. Commun.* **2012**, DOI: 10.1039/C2CC31468A.

(7) Tyson, D. S.; Castellano, F. N. *J. Phys. Chem. A* **1999**, *103*, 10955.

(8) (a) Casadonte, D. J., Jr.; McMillin, D. R. *J. Am. Chem. Soc.* **1987**, *109*, 331. (b) Ford, W. E.; Rodgers, M. A. J. *J. Phys. Chem.* **1992**, *96*, 2917. (c) Leydet, Y.; Bassani, D. M.; Jonusauskas, G.; McClenaghan, N. D. *J. Am. Chem. Soc.* **2007**, *129*, 8688. (d) Yarnell, J. E.; Deaton, J. C.; McCusker, C. E.; Castellano, F. N. *Inorg. Chem.* **2011**, *50*, 7820.

(9) (a) Liao, S.-H.; Shiu, J.-R.; Liu, S.-W.; Yeh, S.-J.; Chen, Y.-H.; Chen, C.-T.; Chow, T. J.; Wu, C.-I *J. Am. Chem. Soc.* **2009**, *131*, 763. (b) Yang, Y.; Cohn, P.; Dyer, A. L.; Eom, S.-H.; Reynolds, J. R.; Castellano, R. K.; Xue, J. *Chem. Mater.* **2010**, *22*, 3580. (c) Zhang, y.; Lai, S.-L.; Tong, Q.-X.; Lo, M.-F.; Ng, T.-W.; Chan, M.-Y.; Wen, Z.-C.; He, J.; Jeff, K.-S.; Tang, X.-L.; Liu, W.-M.; Ko, C.-C.; Wang, P.-F.; Lee, C.-S. *Chem. Mater.* **2012**, *24*, 61.

(10) (a) Yook, K. S.; Lee, J. Y. *Adv. Mater.* **2012**, *24*, 3145. (b) Holmes, R. J.; Forrest, S. R.; Sajoto, T.; Tamayo, A.; Djurovich, P. I.; Thompson, M. E.; Brooks, J.; Tung, Y.-J.; D'Andrade, B. W.; Weaver, M. S.; Kwong, R. C.; Brown, J. J. *Appl. Phys. Lett.* **2005**, *87*, 243507. (c) Chang, C.-F.; Cheng, Y.-M.; Chi, Y.; Chiu, Y.-C.; Lin, C.-C.; Lee, G.-H.; Chou, P.-T.; Chen, C.-C.; Chang, C.-H.; Wu, C.-C. *Angew. Chem., Int. Ed.* **2008**, *47*, 4542. (d) Chiu, Y.-C.; Hung, J.-Y.; Chi, Y.; Chen, C.-C.; Chang, C.-H.; Wu, C.-C.; Cheng, Y.-M.; Yu, Y.-C.; Lee, G.-H.; Chou, P.-T. *Adv. Mater.* **2009**, *21*, 2221. (e) Hsieh, C.-H.; Wu, F.-I.; Fan, C.-H.; Huang, M.-J.; Lu, K.-Y.; Chou, P.-Y.; Yang, Y.-H. O.; Wu, S.-H.; Chen, I.-C.; Chou, S.-H.; Wong, K.-T.; Cheng, C.-H. *Chem.—Eur. J.* **2011**, *17*, 9180.